



Article

Exploring MicroRNAs Associated with Pomegranate Pistil Development: An Identification and Analysis Study

Yujie Zhao ^{1,2}, Jingyi Huang ³, Ming Li ^{1,2}, Hongfang Ren ³, Jian Jiao ^{1,2}, Ran Wan ^{1,2} , Yu Liu ^{1,2}, Miaomiao Wang ^{1,2} , Jiangli Shi ^{1,2} , Kunxi Zhang ^{1,2} , Pengbo Hao ^{1,2}, Shangwei Song ^{1,2}, Tuanhui Bai ^{1,2} and Xianbo Zheng ^{1,2,*}

- ¹ College of Horticulture, Henan Agricultural University, Zhengzhou 450046, China; z1184985369@163.com (Y.Z.); liya1702@163.com (M.L.); jiaojian@henau.edu.cn (J.J.); wanxayl@henau.edu.cn (R.W.); yuliu@henau.edu.cn (Y.L.); wmm2018@henau.edu.cn (M.W.); sjli30@henau.edu.cn (J.S.); kunxi66@163.com (K.Z.); hao_pb@henau.edu.cn (P.H.); songshw959@163.com (S.S.); tuanhuibai88@163.com (T.B.)
- ² Henan Province International Joint Laboratory of Horticultural Plant Biology, Henan Agricultural University, Zhengzhou 450046, China
- ³ College of Forestry, Nanjing Forestry University, Nanjing 210037, China; 19959932089@163.com (J.H.); 17503482685@163.com (H.R.)
- * Correspondence: xbzheng@henau.edu.cn

Abstract: The interaction between miRNAs (microRNAs) and target genes plays an important role in plant pistil development. MiRNAs related to pistils were explored in pomegranate. The differentially expressed miRNAs were screened at different developmental stages of pomegranate pistils, and their target differentially expressed mRNAs were further identified to clarify the regulatory effect of miRNAs on pistil development. In our study, 61 conserved miRNAs were identified in 30 families, including miR395, miR394, miR393, miR161, miR162, and miR168. Among them, miR156, miR157, miR159, miR160, miR164, miR165, miR166, miR167, miR169, and miR172 were involved in the development of flower organs. Eight miRNAs were randomly selected and verified for qRT-PCR analysis. The result analysis indicated that miR160, miR164, and miR172 might be positive factors in the regulation of pomegranate pistil development. MiR156 and miR166 might be involved in regulation of pomegranate pistil development as negative factors.

Keywords: pomegranate; pistil; miRNA; correlation analysis



Citation: Zhao, Y.; Huang, J.; Li, M.; Ren, H.; Jiao, J.; Wan, R.; Liu, Y.; Wang, M.; Shi, J.; Zhang, K.; et al. Exploring MicroRNAs Associated with Pomegranate Pistil Development: An Identification and Analysis Study. *Horticulturae* **2024**, *10*, 85. <https://doi.org/10.3390/horticulturae10010085>

Academic Editor: Xuewu Duan

Received: 30 November 2023

Revised: 10 January 2024

Accepted: 12 January 2024

Published: 16 January 2024



Copyright: © 2024 by the authors. Licensee MDPI, Basel, Switzerland. This article is an open access article distributed under the terms and conditions of the Creative Commons Attribution (CC BY) license (<https://creativecommons.org/licenses/by/4.0/>).

1. Introduction

miRNAs are the class of non-coding small RNAs of eukaryotes genes, most of which are 21–24 nt in length [1,2]. In the nucleus, RNA polymerase II transcribes miRNA genes to generate pri-miRNAs with a stem loop structure and then generates miRNA/miRNA double strands under the action of Dicer enzyme cleavage. Finally, the miRNA strands combine with proteins such as AGO in the cytoplasm to form RNA-induced silencing complexes, which in turn regulate target genes. miRNAs regulate target genes at the post-transcriptional level in two main ways: degrading mRNA or inhibiting protein translation. If the miRNA is fully complementary and paired with its target gene mRNA, the AGO protein bound to miRNA cleaves and degrades the mRNA, resulting in mRNA that cannot be translated [3]. If miRNAs are not highly complementary to the target mRNA, miRNAs bind incompletely to mRNA and inhibit mRNA translation [4]. Plant miRNAs were first reported in *Arabidopsis thaliana* in 2002 [5]. In plants, most miRNAs are exactly matched to target genes, so degradation of mRNAs is the primary way in which miRNAs regulate target genes. miRNAs play important regulatory roles at the post-transcriptional level and participate in the regulation of plant growth and development, including flowering, megasporogenesis, inflorescence, and ovule development [2,6,7]. The *miR2118* mutant

leads to complete male and female sterility [8]. MiR167 regulates its target gene ARFs (auxin response factors), which plays an important role in the development of pistil and stamen groups [9], and miR167 is also involved in regulating the fertility of male and female flowers in *Arabidopsis thaliana* [10]. MiR156 is involved in regulating plant growth cycle transitions [11] and directly inhibits the expression of members of SQUAMOSA promoter binding protein-like (SPL) family, thereby inhibiting the transition from vegetative growth to reproductive growth [12,13]. MiR164 regulates the formation of flower organ boundaries and the boundary formation of lateral organs [14]. The sequences of *miR159* and *miR319* are similar, and the target genes are MYB and TCP transcription factor families, respectively. MiR159-MYB33-ABI5 synergistically regulates the transition of the plant vegetative growth stage [15].

Pomegranate trees produce large numbers of both bisexual flowers that produce fruit and functional male flowers that typically drop and fail to set fruit. Bisexual flowers have a discoid stigma covered with copious exudate, elongated stigmatic papillae, a single elongate style, and numerous and anatropous ovules. In contrast, functional male flowers have reduced female parts and exhibit shortened pistils of variable height. The outer and inner integument primordia form in bisexual flowers with a vertical diameter of 8.1–10.0 mm, and the ovule grows parallel to the nucellus through anticlinal cell division and elongation. However, the integument primordia are not observed in functional male flowers. When the vertical diameter is 10.1–13.0 mm, the outer integument grows rapidly and completely encloses the inner integument in bisexual flowers. Functional male flowers have sterile pistils that show abnormal ovule development. This result indicates that the vertical diameter of 8.1–13.0 mm is a critical stage for pomegranate ovule development [16]. In our study, pomegranate miRNAs of ‘Taishanhong’ bisexual flowers and functional male flowers were sequenced at the critical stages of pomegranate ovule development. miRNAs related to pistil development were mined at the post-transcriptional regulatory level, which laid the foundation for exploring the development mechanism of pomegranate ovules.

2. Materials and Methods

2.1. Plant Materials

According to Zhao’s study [16], pomegranate ovule development was divided into three stages (initial ovule development stage: 5.0–10.0 mm; critical ovule abortion stage: 10.1–13.0 mm; ovule maturity stage: 13.1–18.0 mm). The pistils of bisexual and functional male flowers with vertical bud diameters of 5.0–10.0 mm (I), 10.1–13.0 mm (II), and 13.1–18.0 mm (III) were used as the test materials for miRNAs sequencing. The calyx, petal, and stamen tissues were removed, and only the female organs (ovary, style, and stigma) were retained for mixed-pool transcriptome and miRNA sequencing. The transcriptome data (PRJNA754480) were reported in our previous study [16]. Three biological replicates (18 samples in total) were obtained for each test sample. BF1, BF2, and BF3 represented bisexual flowers’ pistils when their vertical diameters were 5.0–10.0 mm, 10.1–13.0 mm, and 13.1–18.0 mm, respectively. Similarly, MF1, MF2, and MF3 were used to represent functional male flowers’ pistils when their vertical diameters were 5.0–10.0 mm, 10.1–13.0 mm, and 13.1–18.0 mm, respectively.

2.2. Sequencing and Data Analysis

2.2.1. Library Preparation and Sequencing

Total RNA was extracted from pomegranate samples. A total amount of 3 µg of RNA per sample was used as input material for the small RNA library. Sequencing libraries were generated using the NEBNext® Multiplex Small RNA Library Prep Set for Illumina® (NEB, Ipswich, MA, USA) following the manufacturer’s recommendations and index codes were added to attribute sequences of each sample. First strand cDNA was synthesized using M-MuLV Reverse Transcriptase (RNase H⁻). PCR amplification was performed using LongAmp Taq 2X Master Mix, SR Primer for illumina, and index (X) primer. PCR products were purified on 8% polyacrylamide gel (100 V, 80 min). DNA fragments corresponding

to 140–160 bp (the length of small non-coding RNA plus the 3' and 5' adaptors) were recovered and dissolved in 8 μ L of elution buffer. Lastly, library quality was assessed on the Agilent Bioanalyzer 2100 system using DNA High-Sensitivity Chips.

After the library was constructed, Qubit 2.0 was used for preliminary quantification, and the insert size of the library was then detected with Agilent 2100 before the effective concentration of the library was further accurately quantified (>2 nM). The library preparations were sequenced on an Illumina HiSeq 2000 platform and 50 bp single-end reads were generated.

2.2.2. Comparison and Analysis of Raw Data

Clean reads were obtained by deleting the raw reads with splices and low quality. Then, sRNAs in the 18–30 base range were screened from clean reads for subsequent analysis. The small RNA tags were mapped to the pomegranate genome (ASM286412v1) using Bowtie without mismatches to analyze their expression and distribution on the pomegranate genome.

2.2.3. Identification of Conservative miRNA and Novel miRNA

The reads on the pomegranate reference genome were mapped and compared in the miRBase database to obtain the known miRNA secondary structure, sequence, and bases number of sRNA matched on each sample.

miREvo (linux version) [17] and mirdeep2 [18] software were integrated to perform predictive analysis of novel miRNAs in pomegranate.

2.2.4. miRNA Expression and Differential Analysis

The expression levels of known and novel miRNAs in each sample were counted and normalized with TPM (transcripts per million reads) [19]. Normalization formula: normalized expression = mapped readcount/total reads \times 1,000,000.

The sample data analysis was firstly based on the negative binomial distribution of DESeq2 [20], and the difference expression analysis was then performed using the DEGseq R package (1.8.3) [21]. The p -values were adjusted using the Benjamini and Hochberg method. A corrected p -value of 0.05 was set as the threshold for significantly different expression by default.

The heatmap of differential expression of miRNAs was constructed with \log_2 (TPM) values using online software (<http://www.heatmapper.ca/expression/>, accessed on 30 November 2023).

2.2.5. Prediction and Enrichment Analysis of miRNA Target Genes

psRobot_tar in psRobot [22] and targetFinder were used to predict the target genes, and the correspondence between conserved and novel miRNAs and the target genes was analyzed. Gene ontology (GO) and KEGG enrichment analysis were further performed on the target genes.

2.2.6. Correlation Analysis of Sequencing Results

Firstly, the differentially expressed miRNAs were identified, and information regarding the relationship between miRNAs and target genes was further obtained. The differential expression of miRNA and mRNA was analyzed to identify key miRNAs and genes, and the regulatory relationship between miRNAs and target genes was directly displayed through the miRNA–target genes network regulation map. Through the integrated analysis of transcriptome and miRNA sequencing data, the miRNAs involved in regulating the development of pomegranate ovules and their target genes were mined.

2.2.7. qRT-PCR Verification of Sequencing Results

Mature miRNAs were used as the template, *PgActin* was used as a normalizer gene, and the specific primers are shown in Supplemental Table S1 for fluorescence quantitative

verification of sequencing results. The remaining RNA from miRNA sequencing was used for qRT-PCR. Reverse transcription was performed using the PrimeScript™ RT Reagent Kit with gDNA Eraser (Perfect Real Time) (TaKaRa, Osaka, Japan). The primer was designed and synthesized according to the report of Chen et al. [23]. After the primers were mixed, the temperature was set according to Tang et al. [24]. qRT-PCR was performed using SYBR® Premix Ex TAQTii (Tli RNaseH Plus) (TaKaRa, Osaka, Japan). Finally, the PCR analyses were performed on an Applied Biosystems 7500 and the thermal cycler was set as follows: pre-denaturation at 95 °C for 30 s, denaturation at 95 °C for 5 s, and denaturation at 60 °C for 34 s for 40 cycles, with fluorescence then acquired at the second step of each cycle. Dissolution curves were gained as follows: 95 °C for 15 s, 60 °C for 60 s, and 95 °C for 15 s. Three biological and technical replicates were designed for each miRNA. The data were quantitatively analyzed using the $2^{-\Delta\Delta CT}$ method [25]. Data were analyzed using SPSS software 22.0 (IBM, Armonk, NY, USA).

3. Results and Analysis

3.1. Sequencing Results

In this study, the pistils of bisexual flowers and functional male flowers were used as samples to extract RNA. After quality detection, a small RNA library was constructed for sequencing. The raw data obtained by Illumina HiSeq™2500/MiSeq sequencing were uploaded to the NCBI database (PRJNA793612). After filtering, a total of 18 libraries were obtained with the lowest number of clean reads (12,326,514) and the highest number (22,788,789). The GC content ranged from 48 to 54%. In total, 93–97% of the filtered data fragments could be compared to the reference genome (Table 1), indicating that the sequencing results met the requirements for subsequent analysis.

Table 1. Small RNA sequencing data quality and comparison rate statistics.

Sample	Raw Reads	Clean Reads	GC Content (%)	Q20/Q30 (%)	Total sRNA	Mapped sRNA
BF1_1	17,367,419	17,051,495 (98.18%)	49.96	99.04/96.85	14,117,927	94.72%
BF1_2	13,704,093	13,340,571 (97.35%)	50.11	99.39/97.63	8,884,127	94.02%
BF1_3	13,401,810	12,885,356 (96.15%)	50.21	99.29/97.67	7,375,939	95.61%
BF2_1	21,426,062	20,858,435 (97.35%)	49.25	99.31/97.59	17,745,249	94.55%
BF2_2	13,406,968	12,787,925 (95.38%)	49.50	98.48/95.09	10,792,373	96.84%
BF2_3	14,948,932	14,681,792 (98.21%)	49.16	99.05/96.87	11,500,997	94.93%
BF3_1	21,966,339	19,930,652 (90.73%)	50.56	99.15/97.22	14,925,094	96.23%
BF3_2	18,298,780	15,436,529 (84.36%)	50.91	99.24/97.59	5,175,907	97.24%
BF3_3	21,665,923	20,317,773 (93.78%)	50.01	98.07/94.05	18,571,396	95.28%
MF1_1	21,655,951	21,171,252 (97.76%)	48.37	99.41/97.73	16,395,117	92.75%
MF1_2	23,257,849	22,788,789 (97.98%)	49.29	99.41/97.76	19,202,540	93.99%
MF1_3	13,748,317	13,525,096 (98.38%)	49.36	99.33/97.61	10,193,022	94.36%
MF2_1	14,418,240	13,551,334 (93.99%)	51.05	99.43/97.80	6,959,440	95.06%
MF2_2	12,606,612	12,326,514 (97.78%)	50.73	98.21/94.51	6,948,964	93.62%
MF2_3	18,135,526	17,633,277 (97.23%)	49.33	99.11/97.08	14,981,807	96.68%
MF3_1	21,572,493	18,175,437 (84.25%)	49.52	99.13/97.20	15,960,976	94.39%
MF3_2	19,010,757	17,214,821 (90.55%)	51.60	98.91/96.99	10,989,846	97.12%
MF3_3	17,985,939	16,567,891 (92.12%)	53.63	99.31/97.74	4,197,113	96.47%

3.2. Identification and Analysis of Conserved miRNAs and Novel miRNAs

Clean reads were screened, and small RNAs with lengths of 18–30 nt were analyzed, with miRNAs then concentrated at 21–22 nt. A total of 61 conserved miRNAs and 348 novel miRNAs were identified. The 61 conserved miRNAs were identified in 30 families, including *miR395*, *miR394*, *miR393*, *miR161*, *miR162*, and *miR168*. *miR156*, *miR157*, *miR159*, *miR160*, *miR164*, *miR165*, *miR166*, *miR167*, *miR169*, and *miR172* were involved in the development process of plant flower organs (Supplemental Table S2).

Pomegranate miRNA precursors could form the typical stem ring secondary structure, but the number of stem rings formed varies. The first base of most mature sequences was U,

the length of which was concentrated at 20–21 nt, and a few newly identified miRNAs were 24 nt. There were differences in the location of the precursor sequence, such as *miR156*, *miR157*, *novel 104*, and *novel 105* at the 3' end arm and *miR159*, *miR160*, *novel 10*, *novel 100*, *novel 101*, *novel 102*, *novel 107*, and *novel 108* at the 5' end arm (Figure 1). The results showed that the mature bodies of the same family members of pomegranates had the same conserved sequence, and different positions of mature bodies might determine the performance of different functions [26], indicating that different miRNAs members of the same family of pomegranates were functionally conserved and diverse.

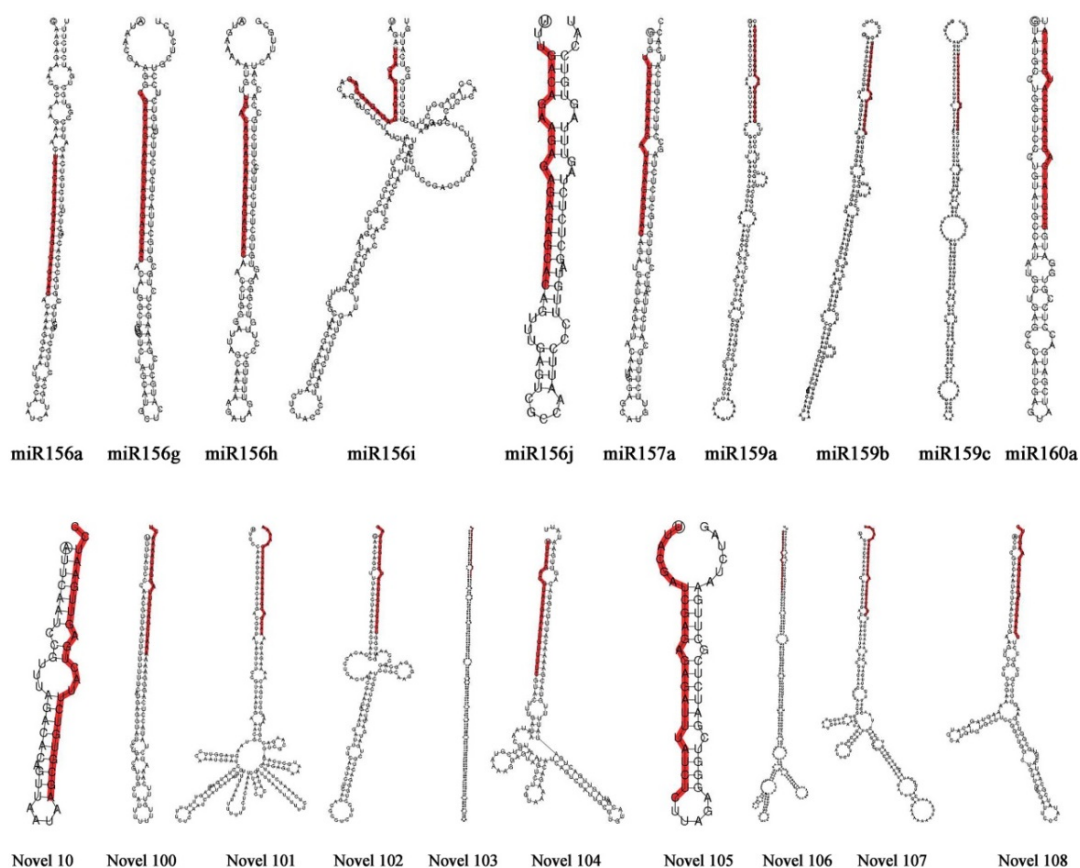


Figure 1. Secondary structure diagram of partial conserved miRNA and novel miRNA. Note: miR represents known microRNA, Novel represents new microRNA. The sequence is the precursor of miRNA, and the red part is the mature sequence.

3.3. miRNA Differential Expression Analysis

Among all pomegranate miRNAs, 76 miRNAs were differentially expressed in the pistil development of bisexual and functional male flowers, including 22 conserved miRNAs and 54 novel miRNAs. A total of 22 miRNAs were differentially expressed at the 5.0–10.0 mm (BF1 vs. MF1) stage, and 51 miRNAs were differentially expressed at the 10.1–13.0 mm (BF2 vs. MF2) stage of pomegranate flowers. A total of 98 miRNAs were expressed differently at different developmental stages of the pistils of bisexual flowers, among which 49 miRNAs were expressed differently between BF2 and BF3. The expression of 26 miRNAs showed significant differences during functional male flower pistil development (Figure 2).

At different pomegranate pistil developmental stages, differentially expressed miRNAs had different expression patterns (Figure 3). Conserved *miR156*, *miR157*, *miR159*, *miR160*, *miR164*, *miR165*, *miR166*, *miR167*, *miR169*, and *miR172* and *novel 41*, *novel 95*, *novel 111*, *novel 178*, *novel 312*, *novel 391*, *novel 437*, and *novel 472* were significantly differentially expressed in pomegranate pistil development (Figure 4). The expression levels of *miR159*,

miR160, *miR164*, *miR167a*, *miR167d*, and *miR172* were significantly higher in bisexual flowers than in functional male flowers. These results indicated that these miRNAs were involved in pomegranate pistil development. However, the expression levels of *miR156*, *miR166a-5p*, *novel 312*, and *novel 437* were significantly higher in functional male flowers than in bisexual flowers, suggesting that these miRNAs might play an important role in pomegranate pistil abortion.

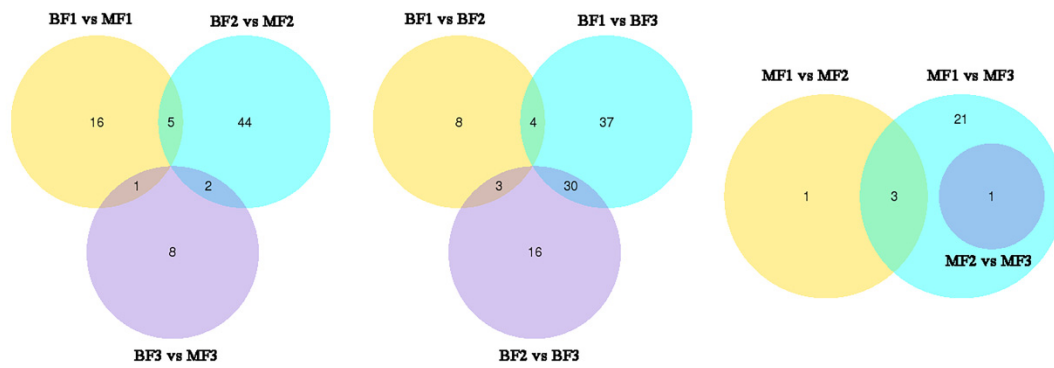


Figure 2. Venn diagram of the differential expression of miRNAs.

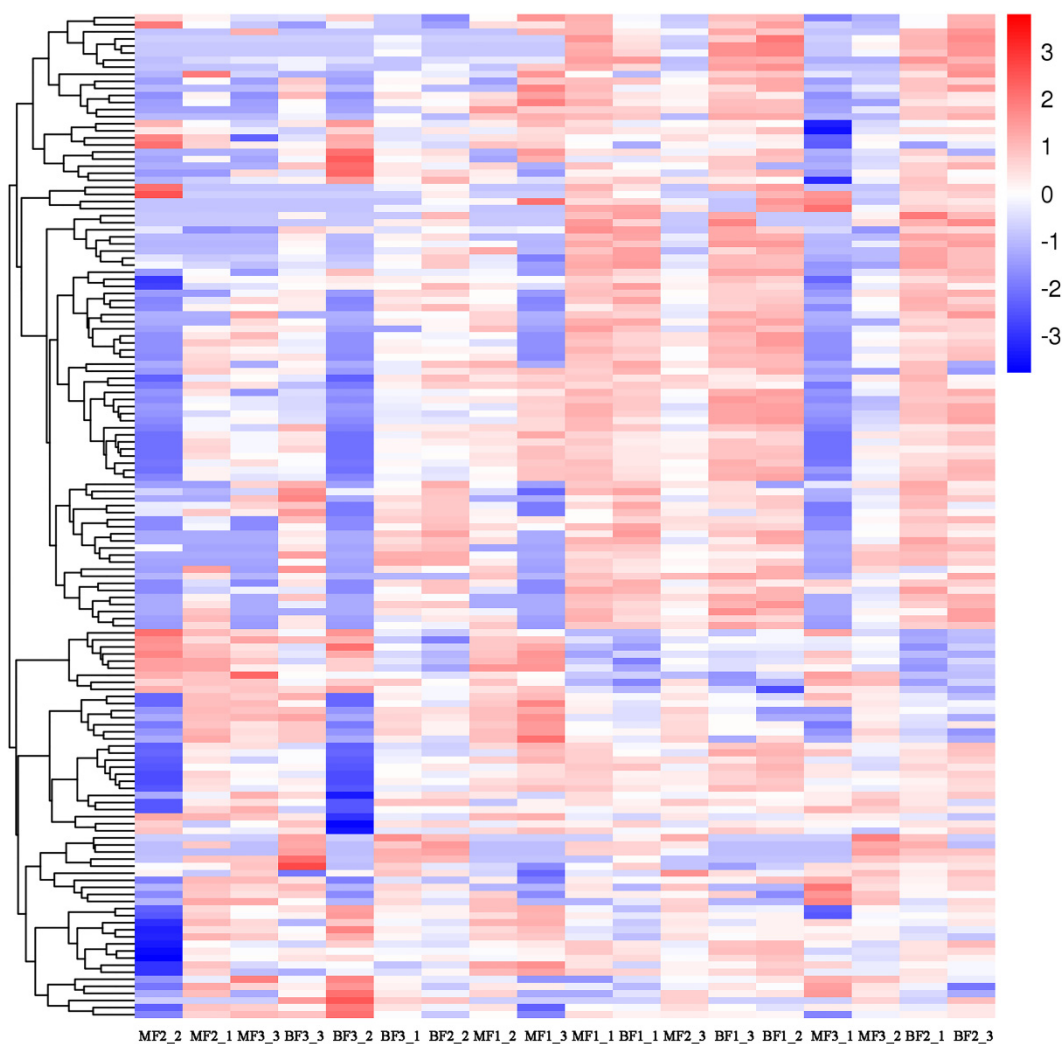


Figure 3. Heat map of differential expression of miRNAs in pomegranate pistils. Note: *_1*, *_2*, and *_3* (such as BF1_1, BF1_2, and BF1_3) represent the three replicates of the sample.

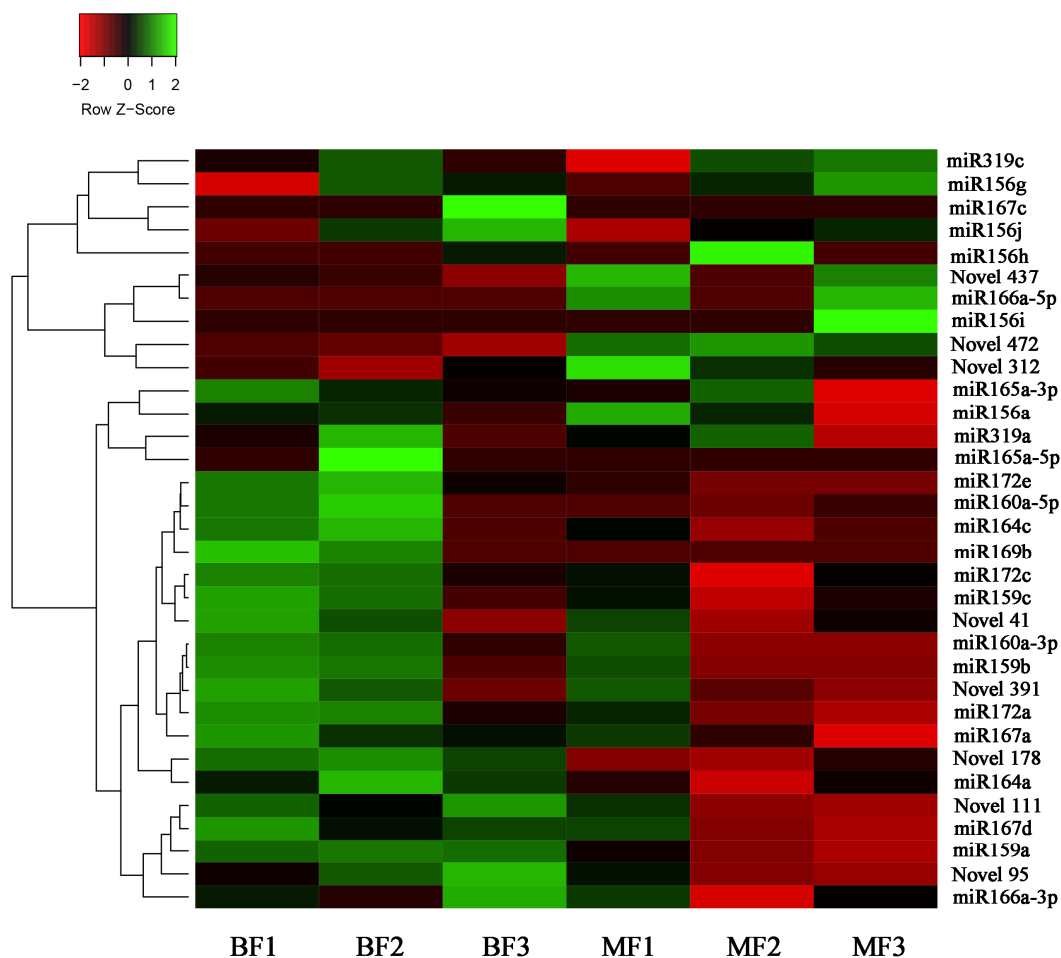


Figure 4. Heat map of conserved miRNAs and novel miRNAs expression patterns in pomegranate pistils.

3.4. miRNA Target Gene Prediction

Pomegranate's 61 known miRNAs and 348 novel miRNAs predicted 4952 and 6932 target genes, respectively. The results of differential expression analysis of miRNAs and target genes indicated that 76 differentially expressed miRNAs predicted 3539 target genes, and some conserved miRNAs and novel miRNAs targeted the same gene (Supplemental Table S3). One miRNA can target multiple target genes, ranging from a few to dozens [27,28]. Our study found that *miR156a-5p* and *miR157a-5p* could target *gene1341*, *gene9689*, *gene2311*, *gene26316*, *gene1095*, and *gene2300*, while *novel 356* and *novel 326* could target *gene26639*. Both *novel 251* and *novel 171* targeted *gene26063*, while *miR172* and *novel 77* were found to target *gene24967*. *PgmiRNA167* identified three target genes (*PgARF6a*, *PgARF6b*, and *PgARF6c*), and *PgARF6a* had a directly targeted regulatory relationship with *PgmiR167a* in pomegranate [29]. According to previous research results, the relationship between pomegranate miRNAs and the target genes will be confirmed in further research.

GO and KEGG function enrichment were performed on the target genes of 76 differentially expressed miRNAs to obtain annotation information for target genes (Supplemental Figure S1). The target genes of differentially expressed miRNAs were mainly annotated to biological processes and molecular functions, including biological regulatory processes (GO:0065007), metabolic processes (GO:0019222), gene expression regulatory biological processes (GO:0010468), protein-binding molecular functions (GO:0005515), and anion binding (GO:0043168). The KEGG function was used to enrich plant hormone signaling, auxin biosynthesis, and BR biosynthesis (Supplemental Figure S2).

3.5. Correlation Analysis of miRNAs and mRNAs

miRNAs regulate target gene expression by binding to complementary sites of target genes to degrade target mRNAs or inhibit their translation [30,31], indicating that miRNAs have a negative correlation with target genes. In our study, correlation analysis of miRNA sequencing and RNA-seq sequencing data was conducted to analyze the expression trend and targeted regulatory relationship between differentially expressed miRNAs and target genes. The statistics of differentially expressed genes as acquired by transcriptome sequencing are shown in Figure 5. The total number of differentially expressed genes was 1722, with 424 genes upregulating expression and 1298 genes downregulating expression. In stage I, 118 genes upregulated and 613 genes downregulated expression. In stage II, 661 genes upregulated and 916 genes downregulated expression. In stage III, 3721 genes upregulated and 3065 genes downregulated expression. As shown in Figure 5, the total number of differentially expressed miRNAs was 76, with 53 miRNAs upregulating expressions and 23 miRNAs downregulating expression. In stage I of pomegranate flower development, 9 miRNAs were upregulated and 22 miRNAs were downregulated. In stage II, 53 miRNAs were upregulated and 5 miRNAs were downregulated. In stage III, 9 miRNAs were upregulated and 9 miRNAs were downregulated.

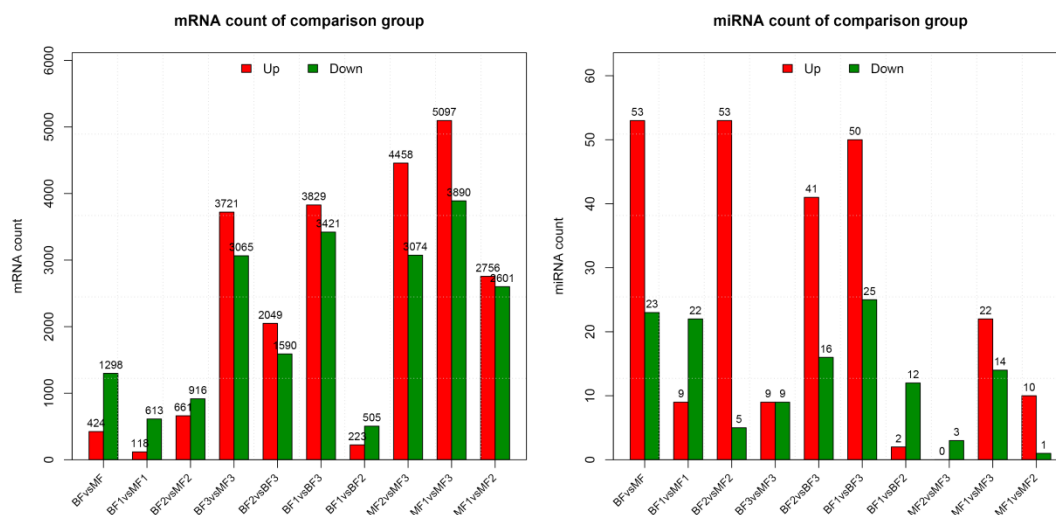


Figure 5. The statistical results of differential expression of mRNA–miRNA in comparison groups. Note: The x-coordinate represents the comparison combination of samples, and the y-coordinate represents the number of differentially expressed mRNA and miRNA in different comparison groups.

Between BF1 and MF1, *miR167a-5p* inhibited the expression of *gene6546*, *gene508*, *gene20506*, and *gene797*, while *miR165a-3p* inhibited *gene8460*. *miR172e-3p* inhibited the expression of *gene9394*, *gene7494*, and *gene22758*. *miR8175* inhibits *gene20953* and *gene20954* expression while promoting *gene1116* expression (Supplemental Figure S3). Between BF2 and MF2, *miR159a*, *miR159b-3p*, and *miR159c* co-inhibited the expression of *gene2996* and *gene10808*. *miR172a*, *miR172c*, and *miR172e-3p* inhibited the expression of *gene10725*, *gene15501*, *gene14955*, and *gene24967*, whereas *miR172a* and *miR172c* promoted *gene8013* expression (Figure 6). *miR164a* and *miR164c-5p* inhibited *gene1312*, *gene18425*, *gene24433*, and *gene25847* expression while promoting the expression of *gene4878*, *gene23729*, *gene21039*, and *gene12163*. During the maturation and development of pomegranate flowers' pistils (13.1–18.0 mm), *novel 111* inhibited the expression of *gene12900*, *gene10203*, *gene3421*, *gene20233*, *gene5397*, *gene10767*, and *gene6293* while promoting *gene6798* expression. Association analysis indicated that *miR164a*, *miR164c-5p*, *miR167a-5p*, *miR172a*, *miR172c*, *miR172e-3p*, and their target genes might be involved in regulating pomegranate pistil development.

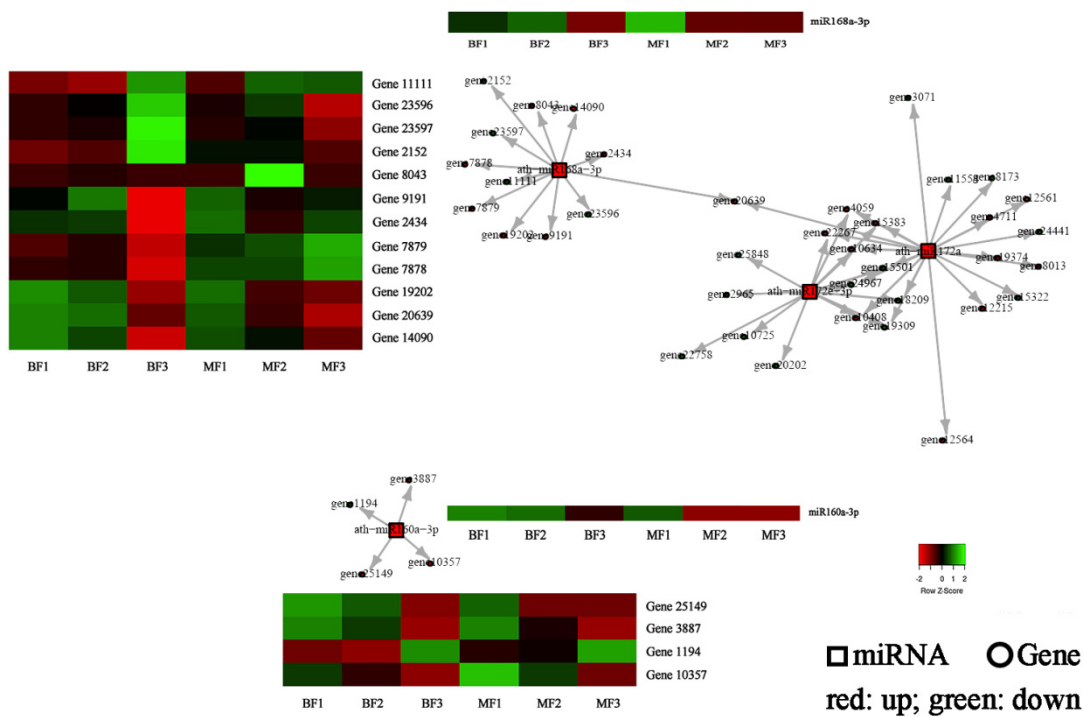


Figure 6. Analysis of the relationship between differentially expressed miR158/miR160/miR172 and target genes. Note: The square represents miRNAs, and the circles represent target genes. Red indicates up-regulated expression, while green represents down-regulated expression.

3.6. qRT-PCR Validation of Differential Transcripts

The qRT-PCR results of miRNA sequencing are shown in Figure 7. In functional male flowers, the expression level of *Pgnovel472* in stage III was higher than that in stages I and II, and the expression level in stage I was the lowest. *Pgnovel472* expression levels in stage III of bisexual flowers were higher than in stages I and II. In functional male flowers, the expression level of *Pgnovel437* in stage I was higher than that in stage II, and the expression of stage III was the lowest. The expression of *Pgnovel437* in stage III of bisexual flowers was five times higher than that in stage I. *Pgnovel178* had a lower expression level in stage II of bisexual flowers. In functional male flowers, the expression of *Pgnovel178* in stage III was higher than that in stages I and II, and the expression in stage I was the lowest.

In bisexual flowers, the expression levels of *PgmiR159a* in stages I and II were lower than in stage III, while the expression in stage II was the lowest. In functional male flowers, *PgmiR159a* expression levels in stages II and III were higher than that in stage I, with the expression in stage II being the highest. The expression level of *PgmiR160a* in stage III of bisexual flowers was higher than that in stage I, and the expression in stage II was the lowest. In functional male flowers, the expression level of *PgmiR160a* at stage II was higher than that at stage I. *PgmiR164c* in bisexual flowers had the highest expression at stage III. The expression level of *PgmiR164c* was the highest at stage II of functional male flower development. The expression of *PgmiR167d* gradually increased in the development of bisexual flowers, with the highest expression level found at stage III. The expression level of *PgmiR167d* was the highest at stage II of functional male flowers. In functional male flowers, the expression level of *PgmiR172e* in stage II was higher than that of stages I and III, with expression at stage I being the lowest. The expression level of *PgmiR172e* was the highest in stage III of bisexual flowers.

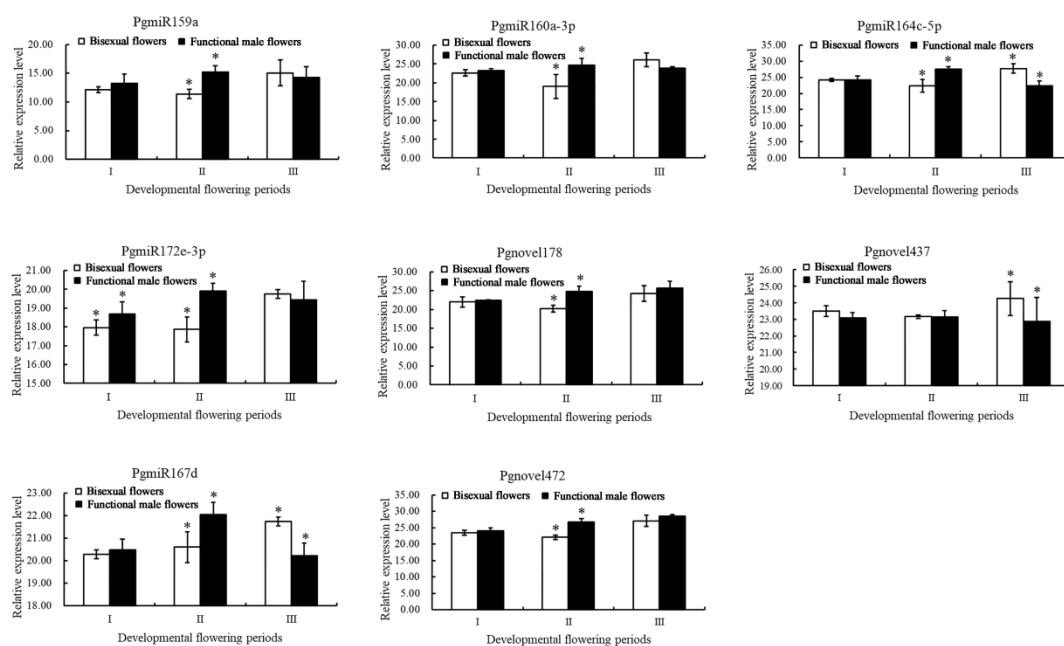


Figure 7. qRT-PCR analysis verified the result of miRNA sequencing. Note: The white bars represent bisexual flowers, and the black bars represent functional male flowers. Data were means \pm SD of three technical replicates. * represents a significance level of $p < 0.05$ in independent sample t -tests.

4. Discussion

miRNAs are involved in flower development processes such as flowering regulation, flower organ morphogenesis, flower organ size and shape, ovule development, and flower organ polarity [7,32–34]. *miR156* can directly inhibit the expression of SPL family members, which control the transition from vegetative stage to reproductive stage. Overexpression of *miR159* and *miR319* causes flower development disorders such as delayed flowering [35]. *miR172* targets *AP2* to control flower organ development [36,37]. Cotton flower organs with *miRNA157* overexpression become smaller with a decreased number of ovules [38]. *miR167* regulates pistil and stamen development in Arabidopsis by targeting *ARF6* and *ARF8* [9]. In our study, a total of 61 conserved miRNAs and 348 novel miRNAs were discovered in the pistils of bisexual flowers and functional male flowers, among which 22 conserved miRNAs and 54 novel miRNAs were differentially expressed. The results of differential expression analysis showed that *miR156*, *miR157*, *miR159*, *miR160*, *miR164*, *miR165*, *miR166*, *miR167*, *miR169*, *miR172*, *novel 41*, *novel 95*, *novel 111*, *novel 178*, *novel 312*, *novel 391*, *novel 437*, and *novel 472* were significantly differentially expressed in the pistil development of bisexual pomegranate flowers and functional male flowers. *Novel 312*, *novel 437*, and *novel 472* were highly expressed in functional male flowers. *Novel 41*, *novel 95*, *novel 111*, and *novel 178* exhibited higher expression in bisexual flowers than in functional male flowers. These results suggest that these differentially expressed novel miRNAs may be involved in regulating pomegranate pistil development.

Apple *mdm-miR156h* was overexpressed in Arabidopsis, resulting in a prolonged juvenile period, increased leaf number, abnormal flower organ development, short horn fruit, and partial seed abortion [13]. Overexpression of populus *miR156j* promoted the development of Arabidopsis rosette leaves, resulting in delayed flowering and negatively regulated target genes *SPL6*, *SPL9*, and *SPL11* [39]. After overexpression of *miR156*, plants showed delayed flowering and decreased fertility under short-day conditions [11]. Our study found that the expression levels of pomegranate *miR156a*, *miR156h*, and *miR156i* in the pistils of functional male flowers were higher than in bisexual flowers, which was consistent with the expression of chestnut *cmo-miR156* in male flower clusters and stamens [40]. However, the expression level of *miR156j* in the pistils of bisexual flowers

was higher than that in functional male flowers. These results indicated that *miR156* is involved in regulating the development of pomegranate pistils.

miR160 targets *ARFs* in ovule development and pollen wall formation [41,42]. Grape *vvi-miR160c/d/e* target *VvARF18* to participate in regulating seed development [43]. Transgenic plants with overexpression of *sly-miR160a* produced tomato fruits with abnormal shape, demonstrating *sly-miR160a* affects early fruit development in tomato by regulating *SLARF10a/10b/17* expression [44,45]. It has been reported that *sly-miR160* regulates the expression of *ARFs* to affect ovary development by regulating auxin polar transport [45]. In our study, it was found that the expression levels of *miR160a-3p* and *miR160a-5p* in the pistils of bisexual flowers were higher than that in functional male flowers, and they were not expressed in the range of 13.1 mm to 18.0 mm. Bisexual flower ovules showed normal development, and functional male flower ovules showed abortion, indicating that *miR160* might be involved in regulating pomegranate ovule development.

During post-harvest storage of strawberry fruits, the expression levels of *fan-miR164d* and *fan-miR164e* were significantly increased, while the expression of *NAC*, their target gene, was downregulated [46,47]. The petals of tomato plants with overexpression of *sly-miR164* did not fall off normally and fruit was seedless [14]. The expression levels of *miR164a* and *miR164c* in the pistils of bisexual flowers were significantly higher than those in functional male flowers, while ovule development was normal in bisexual flowers. These data showed that *miR164* was expressed in pomegranate ovules to maintain normal ovule development.

miR167 targets *ARF6* and *ARF8*, which play an important role in the regulation of the development and maturity of pistil and stamen groups [9]. Overexpression of *miR167* reduces ovule maturity [48]. Our study found that *miR167a* and *miR167d* were expressed in the initial stage of ovule development in bisexual flowers and functional male flowers, while the expression of *miR167c* in the mature stage of the pistils of bisexual flowers was significantly higher than in other developmental stages and in functional male flowers. miRNA target gene prediction showed that *PgmiR167a* and *PgmiR167d* have binding sites on the *PgARF6s* gene sequence [29]. The results showed that *PgmiR167s* regulated *PgARF6s* expression to participate in ovule abortion in pomegranate.

In *Arabidopsis*, *miR172* regulates plant flowering time by regulating the expression of *AP2* (*APETALA2*), which in turn affects flower organ determination and flower morphology [32,49]. *AP2* sequence mutation, which occurs at the *miR172* binding site, results in severe defects in the development of *Arabidopsis* organs [50]. Overexpression of *miR172* in rice causes spikelet loss, flower organ developmental malformation, and decreased fertility [51]. Apple fruit size in transgenic overexpressed *mdm-miR172* plants was significantly reduced [52]. The deletion of *ppe-miR172* binding sites on the peach *AP2* sequence increases the number of peach petals and stamens [53]. The expression of *rch-miR172* was significantly downregulated in the petals, pistils, and stamens of Chinese rose, suggesting that *rch-miR172* may negatively regulate the expression of target gene *AP2* during the development of Chinese rose [54]. *Ach-miR172* targets and regulates *AP2* expression, and the function loss of *ach-miR172* leads to abnormal flower organ development in kiwifruit [55]. The above results show that *miR172* targets *AP2* in the regulation of flower development. Our study found that the expression of *miR172a*, *miR172c*, and *miR172e* in bisexual flowers was higher than in functional male flowers, and they were not expressed at the critical stage of ovule abortion in functional male flowers (10.1 mm–13.0 mm) nor in the mature development of functional male flowers (13.1 mm–18.0 mm). Correlation analysis showed that *miR172* was associated with target genes, which were differentially expressed in pomegranate flowers. These results suggest that *miR172* was involved in regulating the normal development of ovules in pomegranate pistils.

miR167 and *miR165/166* have been shown to be required for integument growth. *miR165/166* is closely related to the formation of meristems in flower organs and in the regulation of meristem activity [56]. Overexpression of *miR165/166* affects flower organ development, such as overexpression of *miR166* in *men1* and *jba-1D* mutants where the

pistils are small and the number of carpels is reduced. *PHB* is involved in ovule primordium morphology and capsular development, and *miR166/165* regulates ovule development by regulating *PHB* expression in the inner ovule primordium [57,58]. *Pg-miR166a-3p* showed significantly higher expression in the pistils of functional male flowers of ‘Tunisian soft seed’ pomegranate than in bisexual flowers. The seed pods of 35S::*Pg-miR166a-3p* transgenic *Arabidopsis thaliana* became smaller, the number of seeds decreased, and the number of flower primordium and plant branches increased [59]. The results showed that the expression of *miR166a-5p* in functional male flowers was higher than that in bisexual flowers, and it was expressed at the critical stage of ovule development. These results suggested that *miR166a-5p* might be involved in regulating pomegranate ovule abortion.

5. Conclusions

After miRNA sequencing and analysis of the three developmental stages of bisexual and functional male pomegranate flowers, it was found that *miR156*, *miR157*, *miR159*, *miR160*, *miR164*, *miR165*, *miR166*, *miR167*, *miR169*, and *miR172* and *novel 41*, *novel 95*, *novel 111*, *novel 178*, *novel 312*, *novel 391*, *novel 437*, and *novel 472* were expressed differently during the pistil development of pomegranate. Target gene prediction, functional enrichment analysis, expression trends, and association analysis of differentially expressed miRNAs showed that *novel 41*, *novel 95*, *novel 111*, *novel 178*, *miR160*, *miR164*, and *miR172* were important regulators involved in the pistil development of pomegranate. *miR160*, *miR164*, and *miR172* might be positive factors in regulation of the pistil development of pomegranate. *miR156* and *miR166* might be involved in regulation of pistil development in pomegranate as negative factors.

Supplementary Materials: The following supporting information can be downloaded at: <https://www.mdpi.com/article/10.3390/horticulturae10010085/s1>, Supplemental Figure S1: Gene ontology-based term classification of different expressed miRNA targets (BF1 vs. MF1); Supplemental Figure S2: Gene ontology-based term classification of different expressed miRNA targets (BF2 vs. MF2 and BF3 vs. MF3); Supplemental Figure S3: Analysis of the relationship between differentially expressed miRNAs and target genes; Supplemental Table S1: The qRT-PCR primer of miRNAs; Supplemental Table S2: Molecular characteristics of partial known and novel miRNAs; Supplemental Table S3: Information for the target genes of partial miRNAs; Supplemental Table S4: Annotation information for differential expression genes of pomegranate.

Author Contributions: Writing—original draft preparation, Y.Z.; writing—review and editing, Y.Z. and J.H.; methodology, M.L.; software, Y.L. and M.W.; validation, J.J. and R.W.; formal analysis, S.S. and T.B.; resources, J.S.; data curation, P.H. and K.Z.; visualization, H.R.; funding acquisition, X.Z. All authors have read and agreed to the published version of the manuscript.

Funding: This work was funded by the fund for modern agricultural industrial technology systems of Henan province (HARS-22-09-Z2).

Data Availability Statement: The transcriptome data (PRJNA754480) and microRNA sequencing data (PRJNA793612) can be downloaded from the NCBI database.

Conflicts of Interest: The authors declare no conflicts of interest.

References

1. Bartel, D.P. MicroRNAs: Genomics, biogenesis, mechanism, and function. *Cell* **2004**, *116*, 281–297. [[CrossRef](#)] [[PubMed](#)]
2. Voinnet, O. Origin, Biogenesis, and Activity of Plant MicroRNAs. *Cell* **2009**, *136*, 669–687. [[CrossRef](#)] [[PubMed](#)]
3. Arribas-Hernández, L.; Kielbinski, L.J.; Brodersen, P. mRNA decay of most *Arabidopsis* miRNA targets requires slicer activity of AGO1. *Plant Physiol.* **2016**, *171*, 2620–2632. [[CrossRef](#)] [[PubMed](#)]
4. Singh, N.K. microRNAs databases: Developmental methodologies, structural and functional annotations. *Interdiscip. Sci.* **2017**, *9*, 357–377. [[CrossRef](#)] [[PubMed](#)]
5. Reinhart, B.J.; Weinstein, E.G.; Rhoades, M.W.; Bartel, B.; Bartel, D.P. MicroRNAs in plants. *Genes Dev.* **2002**, *16*, 1616–1626. [[CrossRef](#)]
6. Khraiweh, B.; Zhu, J.K.; Zhu, J.H. Role of miRNAs and siRNAs in biotic and abiotic stress responses of plants. *Biochim. Biophys. Acta(BBA)-ene Regul. Mech.* **2012**, *1819*, 137–148. [[CrossRef](#)]

7. Petrella, R.; Cucinotta, M.; Mendes, M.A.; Underwood, C.J.; Colombo, L. The emerging role of small RNAs in ovule development, a kind of magic. *Plant Reprod.* **2021**, *34*, 335–351. [[CrossRef](#)]
8. Araki, S.; Le, N.T.; Koizumi, K.; Villar-Briones, A.; Nonomura, K.-I.; Endo, M.; Inoue, H.; Saze, H.; Komiya, R. miR2118-dependent U-rich phasiRNA production in rice anther wall development. *Nat. Commun.* **2020**, *11*, 3115. [[CrossRef](#)]
9. Wu, M.F.; Tian, Q.; Reed, J.W. Arabidopsis microRNA167 controls patterns of ARF6 and ARF8 expression, and regulates both female and male reproduction. *Development* **2006**, *133*, 4211–4218. [[CrossRef](#)]
10. Tan, C.; Zhang, Z.M.; Liu, H.J.; Gao, J.; Rong, Y.Z.; Pan, G.T. Advances on microRNAs regulated flower development of higher plant. *J. Agric. Biotechnol.* **2011**, *19*, 938–952.
11. Schwab, R.; Palatnik, J.F.; Riester, M.; Schommer, C.; Schmid, M.; Weigel, D. Specific effects of microRNAs on the plant transcriptome. *Dev. Cell* **2005**, *8*, 517–527. [[CrossRef](#)] [[PubMed](#)]
12. Klein, J.; Saedler, H.; Huijser, P. A new family of DNA binding proteins includes putative transcriptional regulators of the *Antirrhinum majus* floral meristem identity gene *SQUAMOSA*. *Mol. Genet. Genom.* **1996**, *250*, 7–16. [[CrossRef](#)]
13. Sun, C.; Zhao, Q.; Liu, D.D.; You, C.X.; Hao, Y.J. Ectopic expression of the apple Md-miRNA156h gene regulates flower and fruit development in Arabidopsis. *Plant Cell* **2013**, *112*, 343–351. [[CrossRef](#)]
14. Yang, C.W. MiR164 is Required for Tomato Flower Initiation and Fruit Development. Master's Thesis, Chongqing University, Chongqing, China, 2012.
15. Guo, C.; Jiang, Y.; Shi, M.; Wu, X.; Wu, G. *ABI5* acts downstream of miR159 to delay vegetative phase change in Arabidopsis. *New Phytol.* **2021**, *231*, 339–350. [[CrossRef](#)] [[PubMed](#)]
16. Zhao, Y.; Wang, Y.; Yan, M.; Liu, C.; Yuan, Z. *BELL1* interacts with *CRABS CLAW* and *INNER NO OUTER* to regulate ovule and seed development in pomegranate. *Plant Physiol.* **2023**, *191*, 1066–1083. [[CrossRef](#)] [[PubMed](#)]
17. Wen, M.; Shen, Y.; Shi, S.; Tang, T. miREvo: An integrative microRNA evolutionary analysis platform for next-generation sequencing experiments. *BMC Bioinform.* **2012**, *13*, 140. [[CrossRef](#)]
18. Friedländer, M.R.; Mackowiak, S.D.; Li, N.; Chen, W.; Rajewsky, N. miRDeep2 accurately identifies known and hundreds of novel microRNA genes in seven animal clades. *Nucleic Acids Res.* **2011**, *40*, 37–52. [[CrossRef](#)]
19. Zhou, L.; Chen, J.; Li, Z.; Li, X.; Hu, X.; Huang, Y.; Zhao, X.; Liang, C.; Wang, Y.; Sun, L.; et al. Integrated Profiling of MicroRNAs and mRNAs: MicroRNAs Located on Xq27.3 Associate with Clear Cell Renal Cell Carcinoma. *PLoS ONE* **2010**, *5*, e15224. [[CrossRef](#)]
20. Love, M.I.; Huber, W.; Anders, S. Moderated estimation of fold change and dispersion for RNA-seq data with DESeq2. *Genome Biol.* **2014**, *15*, 550. [[CrossRef](#)]
21. Wang, L.; Feng, Z.; Wang, X.; Wang, X.; Zhang, X. DEGseq: An R package for identifying differentially expressed genes from RNA-seq data. *Bioinformatics* **2010**, *26*, 136–138. [[CrossRef](#)]
22. Wu, H.J.; Ma, Y.-K.; Chen, T.; Wang, M.; Wang, X.J. PsRobot: A web-based plant small RNA meta-analysis toolbox. *Nucleic Acids Res.* **2012**, *40*, 22–28. [[CrossRef](#)]
23. Chen, C.; Ridzon, D.A.; Broomer, A.J.; Zhou, Z.; Lee, D.H.; Nguyen, J.T.; Barbisin, M.; Xu, N.L.; Mahuvakar, V.R.; Andersen, M.R.; et al. Real-time quantification of microRNAs by stem-loop RT-PCR. *Nucleic Acids Res.* **2005**, *33*, e179. [[CrossRef](#)] [[PubMed](#)]
24. Tang, F.; Hajkova, P.; Barton, S.C.; Lao, K.; Surani, M.A. MicroRNA expression profiling of single whole embryonic stem cells. *Nucleic Acids Res.* **2006**, *34*, e9. [[CrossRef](#)] [[PubMed](#)]
25. Livak, K.J.; Schmittgen, T.D. Analysis of relative gene expression data using realtime quantitative PCR and the 2- $\Delta\Delta$ CT method. *Methods* **2001**, *25*, 402–408. [[CrossRef](#)]
26. Mi, S.; Cai, T.; Hu, Y.; Chen, Y.; Hodges, E.; Ni, F.; Wu, L.; Li, S.; Zhou, H.; Long, C.; et al. Sorting of small RNAs into *Arabidopsis* Argonaute complexes is directed by the 5' terminal nucleotide. *Cell* **2008**, *133*, 116–127. [[CrossRef](#)] [[PubMed](#)]
27. Jones-Rhoades, M.W.; Bartel, D.P. Computational identification of plant microRNAs and their targets, including a stress-induced miRNA. *Mol. Cell* **2004**, *14*, 787–799. [[CrossRef](#)]
28. Jones-Rhoades, M.W.; Bartel, D.P.; Bartel, B. MicroRNAs and their regulatory roles in plants. *Annu. Rev. Plant Biol.* **2006**, *57*, 19–53. [[CrossRef](#)]
29. Zhao, Y.; Wang, Y.; Zhao, X.; Yan, M.; Ren, Y.; Yuan, Z. ARF6s identification and function analysis provide insights into flower development of *Punica granatum* L. *Front. Plant Sci.* **2022**, *13*, 833747. [[CrossRef](#)]
30. Kurihara, Y.; Watanabe, Y. Arabidopsis micro-RNA biogenesis through Dicer-like 1 protein functions. *Proc. Natl. Acad. Sci. USA* **2004**, *101*, 12753–12758. [[CrossRef](#)]
31. Filipowicz, W.; Bhattacharyya, S.N.; Sonenberg, N. Mechanisms of post-transcriptional regulation by microRNAs: Are the answers in sight? *Nat. Rev. Genet.* **2008**, *9*, 102–114. [[CrossRef](#)]
32. Allen, R.S.; Li, J.; Stahle, M.I.; Dubroué, A.; Gubler, F.; Millar, A.A. Genetic analysis reveals functional redundancy and the major target genes of *Arabidopsis* miR159 family. *Proc. Natl. Acad. Sci. USA* **2007**, *104*, 16371–16376. [[CrossRef](#)] [[PubMed](#)]
33. Aukerman, M.J.; Sakai, H. Regulation of flowering time and floral organ identity by a microRNA and its APETALA2-like target genes. *Plant Cell* **2003**, *15*, 2730–2741. [[CrossRef](#)] [[PubMed](#)]
34. Zhang, Q.W.; Yang, X.H.; Li, F.; Deng, Y.T. Advances in miRNA-mediated growth and development regulation in horticultural crops. *Acta Hort. Sin.* **2022**, *49*, 1145–1161.

35. Palatnik, J.F.; Wollmann, H.; Schommer, C.; Schwab, R.; Boisbouvier, J.; Rodriguez, R.; Warthmann, N.; Allen, E.; Dezulian, T.; Huson, D.; et al. Sequence and expression differences underlie functional specialization of *Arabidopsis* MicroRNAs miR159 and miR319. *Dev. Cell* **2007**, *13*, 115–125. [[CrossRef](#)] [[PubMed](#)]
36. Wu, G.; Poethig, R.S. Temporal regulation of shoot development in *Arabidopsis thaliana* by Mir156 and its target SPL3. *Development* **2006**, *133*, 3539–3547. [[CrossRef](#)] [[PubMed](#)]
37. Wu, G.; Park, M.Y.; Conway, S.R.; Wang, J.-W.; Weigel, D.; Poethig, R.S. The sequential action of miR156 and miR172 regulates developmental timing in *Arabidopsis*. *Cell* **2009**, *138*, 750–759. [[CrossRef](#)] [[PubMed](#)]
38. Liu, N.; Tu, L.; Wang, L.; Hu, H.; Xu, J.; Zhang, X. MicroRNA 157-targeted SPL genes regulate floral organ size and ovule production in cotton. *BMC Plant Biol.* **2017**, *17*, 7. [[CrossRef](#)]
39. Duan, Z.X. Expression Pattern and Functional Analysis of microRNA Peu-miR156j and Peu-miR169 from *Populus euphratica*. Master's Thesis, Beijing Forestry University, Beijing, China, 2012.
40. Chen, G.; Li, J.; Liu, Y.; Zhang, Q.; Gao, Y.; Fang, K.; Cao, Q.; Qin, L.; Xing, Y. Roles of the GA-mediated SPL gene family and miR156 in the floral development of Chinese chestnut (*Castanea mollissima*). *Int. J. Mol. Sci.* **2019**, *20*, 1577. [[CrossRef](#)]
41. Liu, X.D.; Zhang, H.; Zhao, Y.; Feng, Z.Y.; Li, Q.; Yang, H.Q.; Luan, S.; Li, J.M.; He, Z.H. Auxin controls seed dormancy through stimulation of abscisic acid signaling by inducing ARF-mediated ABI3 activation in *Arabidopsis*. *Proc. Natl. Acad. Sci. USA* **2013**, *110*, 15485–15490. [[CrossRef](#)]
42. Wu, S.C. Functional Characterization of mir160 in Cotton Ovule Development. Master's Thesis, Huazhong Agricultural University, Wuhan, China, 2016.
43. Bai, Y.H.; Wang, W.R.; Dong, T.Y.; Guan, L.; Su, Z.W.; Jia, H.F.; Fang, J.G.; Wang, C. vvi-miR160s in mediating vvARF18 response to gibberellin regulation of grape seed development. *Sci. Agric. Sin.* **2020**, *53*, 1890–1903.
44. Hendelman, A.; Buxdorf, K.; Stav, R.; Kravchik, M.; Arazi, T. Inhibition of lamina outgrowth following *Solanum lycopersicum* auxin response factor 10 (SIARF10) derepression. *Plant Mol. Biol.* **2012**, *78*, 561–576. [[CrossRef](#)] [[PubMed](#)]
45. Damodharan, S.; Zhao, D.Z.; Arazi, T. A common mi RNA160-based mechanism regulates ovary patterning, floral organ abscission and lamina outgrowth in tomato. *Plant J.* **2016**, *86*, 458–471. [[CrossRef](#)] [[PubMed](#)]
46. Li, J.; Lai, T.; Song, H.; Xu, X. MiR164 is involved in delaying senescence of strawberry (*Fragaria ananassa*) fruit by negatively regulating NAC transcription factor genes under low temperature. *Russ. J. Plant Physiol.* **2017**, *64*, 251–259. [[CrossRef](#)]
47. Zhang, X.; Wang, M.; Gan, C.; Ren, Y.; Zhao, X.; Yuan, Z. Riboflavin application delays senescence and relieves decay in harvested strawberries during cold storage by improving antioxidant system. *LWT-Food Sci. Technol.* **2023**, *182*, 114810. [[CrossRef](#)]
48. Ru, P.; Xu, L.; Ma, H.; Huang, H. Plant fertility defects induced by the enhanced expression of microRNA167. *Cell Res.* **2006**, *16*, 457–465. [[CrossRef](#)]
49. Jung, J.H.; Seo, Y.H.; Seo, P.J.; Reyes, J.L.; Yun, J.; Chua, N.-H.; Park, C.-M. The GIGANTEA-regulated microRNA172 mediates photoperiodic flowering Independent of CONSTANS in *Arabidopsis*. *Plant Cell* **2007**, *19*, 2736–2748. [[CrossRef](#)]
50. Grigorova, B.; Mara, C.; Hollender, C.; Sijacic, P.; Chen, X.; Liu, Z. LEUNIG and SEUSS co-repressors regulate miR172 expression in *Arabidopsis* flowers. *Development* **2011**, *138*, 2451–2456. [[CrossRef](#)]
51. Zhu, Q.-H.; Upadhyaya, N.M.; Gubler, F.; Helliwell, C.A. Over-expression of miR172 causes loss of spikelet determinacy and floral organ abnormalities in rice (*Oryza sativa*). *BMC Plant Biol.* **2009**, *9*, 149. [[CrossRef](#)]
52. Yao, J.; Xu, J.; Cornille, A.; Tomes, S.; Karunairetnam, S.; Luo, Z.; Bassett, H.; Whitworth, C.; Rees-George, J.; Ranatunga, C.; et al. A microRNA allele that emerged prior to apple domestication may underlie fruit size evolution. *Plant J.* **2015**, *84*, 417–427. [[CrossRef](#)]
53. Gattolin, S.; Cirilli, M.; Pacheco, I.; Ciacciulli, A.; Linge, C.D.S.; Mauroux, J.; Lambert, P.; Cammarata, E.; Bassi, D.; Pascal, T.; et al. Deletion of the miR172 target site in a TOE-type gene is a strong candidate variant for dominant double-flower trait in Rosaceae. *Plant J.* **2018**, *96*, 358–371. [[CrossRef](#)]
54. Sui, M.J.; Yan, H.J.; Wang, Z.Z.; Qiu, X.Q.; Jian, H.Y.; Wang, Q.G.; Chen, M.; Zhang, H.; Tang, K.X. Identification of microRNA associated with flower organ development in *Rosa chinensis* 'Viridiflora'. *Plant Sci. J.* **2019**, *37*, 37–46.
55. Varkonyi-Gasic, E.; Lough, R.H.; Moss, S.M.A.; Wu, R.; Hellens, R.P. Kiwifruit floral gene APETALA2 is alternatively spliced and accumulates in aberrant indeterminate flowers in the absence of miR172. *Plant Mol. Biol.* **2012**, *78*, 417–429. [[CrossRef](#)]
56. Zhang, X.; Henderson, I.R.; Lu, C.; Green, P.J.; Jacobsen, S.E. Role of RNA polymerase IV in plant small RNA metabolism. *Proc. Natl. Acad. Sci. USA* **2007**, *104*, 4536–4541. [[CrossRef](#)]
57. Sieber, P.; Gheyselinck, J.; Gross-Hardt, R.; Laux, T.; Grossniklaus, U.; Schneitz, K. Pattern formation during early ovule development in *Arabidopsis thaliana*. *Dev. Biol.* **2004**, *273*, 321–334. [[CrossRef](#)]
58. Hashimoto, K.; Miyashima, S.; Sato-Nara, K.; Yamada, T.; Nakajima, K. Functionally diversified members of the miR165/6 gene family regulate ovule morphogenesis in *Arabidopsis thaliana*. *Plant Cell Physiol.* **2018**, *59*, 1017–1026. [[CrossRef](#)]
59. Chen, L.N. Identification of microRNAs Involved in Pomegranate Female Sterility and Functional Analysis on the Regulation of Pg-miR166a-3p on Pistil Development. Ph.D. Thesis, Chinese Academy of Agricultural Sciences, Beijing, China, 2020.

Disclaimer/Publisher's Note: The statements, opinions and data contained in all publications are solely those of the individual author(s) and contributor(s) and not of MDPI and/or the editor(s). MDPI and/or the editor(s) disclaim responsibility for any injury to people or property resulting from any ideas, methods, instructions or products referred to in the content.